Arboriculture & Urban Forestry 2012. 38(6): 277–286

An Evaluation of Internal Defects and Their Effect on Trunk Surface Temperature in *Casuarina equisetifolia* L. (Casuarinaceae)

Daniel C. Burcham, Eng-Choon Leong, Yok-King Fong, and Puay-Yok Tan

Abstract. Tree risk assessment is important when communities choose to cultivate trees near people and property, and many tools may be used to enhance these assessments. The effectiveness of determining internal tree stem condition by measuring trunk surface temperatures with infrared cameras was assessed in this study. The trunk surface temperature of 48 *Casuarina equisetifolia* was evaluated; the trees were felled and dissected to quantify internal stem defects; and a mixed-methods approach was employed to determine the presence of defects. In total, 27% of trees were decayed, 62% discolored, 6% cavitated by termite infestations, and 2% undamaged. Qualitative visual evaluation of the infrared images revealed the close association of external stem features, opposed to internal defects, with surface temperature distributions. External features, such as cankers, detached bark, and mechanical damage, were associated with temperature anomalies. The trees' internal condition accounted for a small percentage of the variability in evaluated temperature measurements ($r^2 = 0.001$-0.096). Overall, no clear relationship was found between the extent of internal defects and surface temperature distributions. These results are practically important for the arboricultural professional community because they show the technique does not provide accurate results about the internal condition of trees.

Key Words. *Casuarina equisetifolia*; Diagnostic Device; Infrared Camera; Internal Defect; Singapore; Temperature; Thermal.

In managing urban forests, arborists strive to maximize the environmental, social, and economic benefits of trees while minimizing costs to society. These costs may include direct financial resources used to plant and maintain trees as well as indirect socioeconomic costs resulting from undesirable conflicts with trees, such as root growth into sewer pipes, drains, and pavement. The costs of structural tree failures, in particular, represent an important challenge toward mitigating damage to property and injury to people. In general, trees naturally adapt to external forces experienced cumulatively on-site with various anatomical features, including reaction (i.e., tension and compression) wood (Fisher and Stevenson 1981), buttress roots (Setten 1953), mass damping of flexible branches (James et al. 2006), and wood material property optimization (Wiemann and Williamson 1989; Dahle and Grabosky 2010). However, trees fail when loaded by an external force exceeding the structural capacity of their material components; these critical forces are commonly generated by intense weather events, including wind, rain, ice, and snow.

Structural defects can render trees less resilient against external forces, and those trees containing defects in an urban setting may become hazardous (Harris et al. 2003). Structural defects in the stem and branches commonly include cracks, lightning scars, included bark, cankers, cavities, and decayed wood; these defects can substantially reduce the load-bearing capacity of the natural structure. Consequently, arborists regularly conduct tree risk assessments to evaluate the condition of individual trees, search for the existence of structural defects, and, if necessary, perform corrective work to preserve their long-term condition (Smiley et al. 2000). The ultimate objective of a tree risk assessment is to recognize and remedy hazardous specimens before failure and damage occurs; this process requires that arborists successfully recognize and identify many different structural defects (Matheny and Clark 1994).

Frequently, arborists use visual tree inspection frameworks to guide the tree risk assessment process (Matheny and Clark 1994; Mattheck and Breloer 1994; Ellison 2005). These frameworks ensure a consistent, systematic approach toward visually observing a tree's general and local condition for possible defects. Despite these professional best practices, wood decay, in contrast with many other defects, can remain obscure during an inspection in the absence of external symptoms. Symptoms indicative of wood decay, such as fruiting bodies, cracks, fiber buckling, and crown dieback, may not be visible until the advanced stages of infection (Schwarze et al. 2004). A complete review of the epidemiology, diagnosis, and assessment of wood decay in trees can be found elsewhere (Rayner and Boddy 1988; Schwarze 2008).

In some cases, visual symptoms can point to the probable existence of wood decay, but they may not permit accurate estimates of an infection's extent or severity. The supplemental use of advanced tree diagnostic devices has received considerable research attention in order to enhance wood decay assessment. The devices enhance visual tree inspections by employing optical, acoustic, electrical, mechanical, or biochemical measurement techniques to distinguish material property changes

associated with decayed wood inside the stem (Schwarze et al. 1997; Costello and Quarles 1999; Larsson et al. 2004; Rabe et al. 2004; Nicolotti et al. 2009; Johnstone et al. 2010). Wood decay infections cause measurable changes to the physical, mechanical, chemical, and biological wood properties evaluated by the devices, including low density and altered moisture relations (Cartwright and Findlay 1958). However, the devices vary considerably in terms of their accuracy, speed of measurement, and invasiveness (Ouis 2003; Kersten and Schwarze 2005).

The use of infrared (IR) cameras as tree diagnostic devices has been proposed as a non-destructive and rapid technique for assessing internal defects, including wood decay (Catena 2003). The principles, advantages, and disadvantages of the technique have been extensively reviewed (Catena and Catena 2008). Principally, the technique attempts to associate changes in the thermal properties of wood containing defects with surface temperature anomalies (Catena et al. 1990). In this method, the trunk surface temperature of trees is captured using IR cameras. The relatively low density, structural discontinuity, and altered moisture content of internal defects modify the wood's thermal properties, including thermal conductivity, capacity, and diffusivity (Scheffer 1936). These material property changes may, under certain environmental conditions, render trunk surface temperature anomalies observable in the IR image. The earliest publications reported that trunk surface temperatures were highly variable and relatively cooler at locations overlying internal defects (Catena et al. 1990). Although initial attempts to verify the technique relied heavily on qualitative case studies, recent research efforts have evaluated the technique using quantitative measurement and analysis approaches (Bellett-Travers and Morris 2010; Burcham et al. 2011).

In particular, Burcham et al. (2012) found that relatively large internal defects, occupying at least 76% of the stem cross-sectional area (CSA), were required to produce a measurable reduction in surface temperature under controlled conditions. Similarly, Bellett-Travers and Morris (2010) reported that surface temperature was most correlated (r^2 = 0.31 - 0.55) with the radial wood thickness exclusively in trees containing a distinct, compartmentalized internal cavity. The relationship between these features was not present in healthy specimens or those containing incipient decay (Bellett-Travers and Morris 2010). Collectively, these results suggest that the IR camera technique may effectively identify a narrow range of relatively large internal defects.

The potential diagnostic advantages offered by the IR camera technique could be significant in urban areas. First, there is some evidence showing that wounds created by invasive diagnostic tools serve as infection courts for wood decay fungi (Kersten and Schwarze 2005), and the non-invasive infrared camera measurements could provide an alternative. Second, the IR camera offers comparatively quick measurement speeds. Third, the broad spatial orientation of the IR image could provide information about larger areas of the trunk. However, research clarifying the resolution and accuracy of this technique is needed. This study was designed to: 1) evaluate the relationship between the internal defects and surface temperature measurements collected with an IR camera, and 2) evaluate methods of interpreting the IR images using qualitative and quantitative data analysis techniques.

MATERIALS AND METHODS

Selection of Plant Material

Forty-eight *Casuarina equisetifolia* were selected from a sandy coastal forest situated at the eastern edge of Singapore (lat. 1°20'51.33"N, long. 103°59'53.45"E) for inclusion in this study. The study area was populated, principally, by this actinorhizal pioneer species, occasionally supplanted by the coastal species *Terminalia catappa* L. (Combretaceae) and the non-native pioneer *Acacia auriculiformis* A. Cunn. ex Benth. (Leguminosae). The trees were growing on reclaimed land originally formed in 1991 by the deposition of marine sand, dredged from the seabed and containing less than 10% fines, on top of a highly compressible layer of Singapore marine clay (Bo et al. 2005). Trees were selected for study based on the satisfaction of at least one pre-defined criterion, including 1) external decay associated signs and symptoms, or 2) a stem diameter, exceeding 40 cm, measured at 1 m above the ground. After selection, the trees were assigned a unique alphabetic label and marked with high-visibility plastic tape. This tape increased visibility of the selected trees in the forest and served as a tag for subsequent experimental work. Height (m), diameter (cm), and geospatial position (latitude and longitude) were measured and recorded (Figure 1).

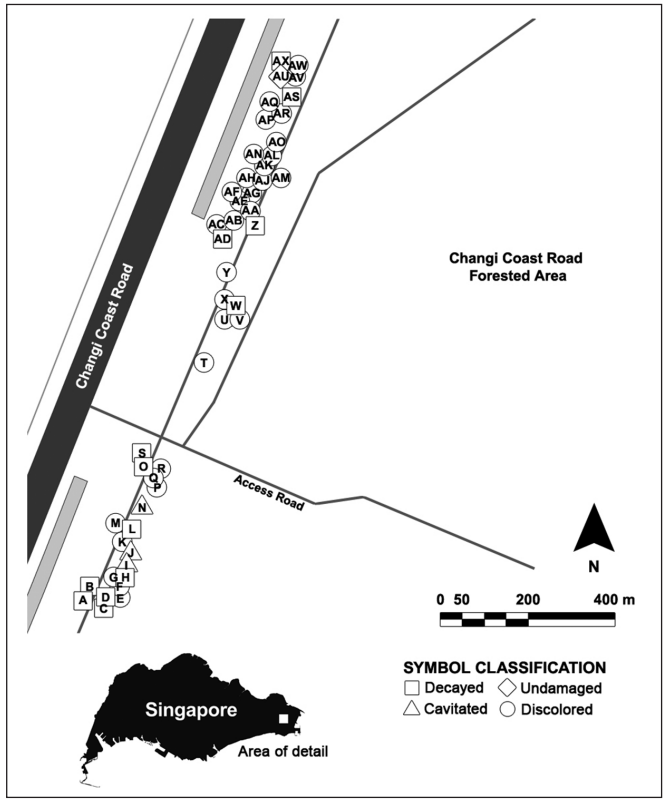

Figure 1. The 48 sampled *Casuarina equisetifolia* were measured with an infrared camera and removed for study from an early successionary coastal forest situated at the eastern edge of Singapore (1°20'51.33"N 103°59'53.45"E).

Collection of Infrared Images

Infrared images were collected using a Thermoteknix VisIR 640 IR camera (Cambridge, UK) calibrated using ambient temperature and emissivity values appropriate for tree bark prior to evaluation. The emissivity setting was held constant at 0.95, an average of six bark emissivity values for temperate species reported by Salisbury and D'Aria (1992), and the ambient temperature was adjusted for each image to correspond with conditions at the time of collection. The camera was consistently positioned 1.2 m above the ground at a distance of 10 m from the trunk base and oriented to measure the surface temperature on each tree's western aspect (270°C). The images were collected for all 48 trees between 2:00 and 4:00 pm on March 5, 2011. The camera orientation and time of image collection were selected to ensure each tree received the maximum solar heating. During this process, the marking tape was removed from each tree immediately before measurement and afterwards replaced. Climate data for the immediate area during the same period was obtained from the Meteorological Services Division, National Environment Agency, Singapore.

Destructive Harvesting and Measurement

After measurement, the trees were felled and the lowest 3 m of the trunk was removed and retained for dissection. These 3 m trunk sections were cut with a chainsaw into 15, 20 cm thick cross sections. Each cross section was examined for bark color and texture, cavitations, reaction zones, sapwood, and heartwood. Each cross section was photographed for visual reference within a 1 m × 1 m square frame, containing a metric scale on two opposing axes (Figure 2).

The presence of decayed wood was confirmed by measuring the axial compressive strength of fungal lesions using a method modified from Watson (2008). A Penetrometer® (Lang Penetrometer, Gulf Shores, Alabama, U.S.) fitted with a blunt dissecting probe was used to exert 83 N of force axially onto the cut wood surface, and the depth of holes created by the probe was measured using a Digimatic Caliper (Mitutoyo Corporation, Kawasaki, Japan). Using this method, fungal lesions permitting impressions at least 1 mm greater than proximal healthy tissue was considered decayed.

The stem perimeter and outline of internal defects (e.g., decay, discoloration, cavitation) were traced manually onto a clear plastic transparency sheet from the superior cut surface of each cross section. In addition, tracings were also made from the remaining flush cut stumps *in situ*, yielding the lowest measurement from 16 total cross-sectional tracings spaced equidistantly along the 3 m section. The tracings were digitized using a flatbed scanner and the CSA of each feature was determined using the image analysis toolset in Photoshop® CS3 Extended (Adobe Systems, San Jose, California, U.S.). These values were subsequently used to determine the relative defect CSA (%) for six defect categories, including 1) undamaged, 2) discolored, 3) decayed, 4) decayed + discolored, 5) cavitated, and 6) cavitated + discolored (Figure 3).

Data Analysis

The collected data were analyzed using a concurrent mixed-methods approach to corroborate findings obtained from both qualitative and quantitative strategies. IR images were processed using the TherMonitor® Reporter System (Thermoteknix 2001). The temperature span rendered in each image was set between 25°C and 35°C, and the captured images were compared visually for

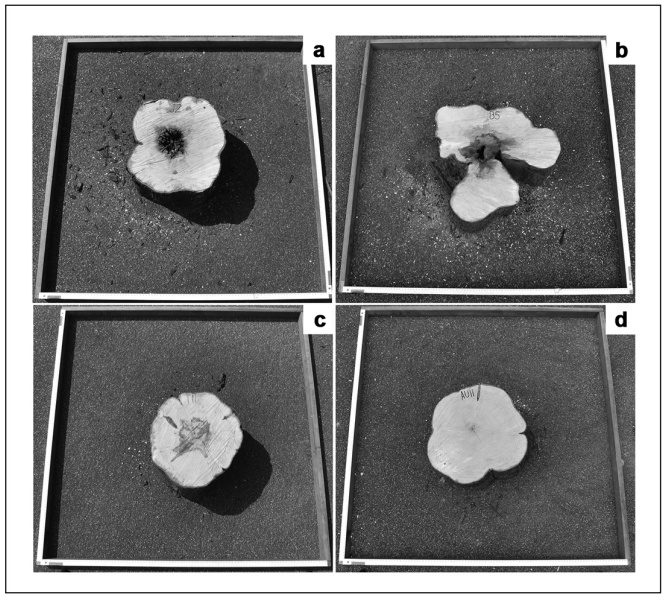

Figure 2. Each cross section was photographed in a 1 m × 1 m frame for visual reference. Among the sampled trees, sections were excised containing: (a) termite-induced cavitations with irregular, smooth-walled voids; (b) decay with irregular color changes, host reaction zones, and dark fungal interaction lines; (c) discoloration with irregular wood color changes and dark fungal interaction lines; and (d) no measurable defects with substantially healthy tissue.

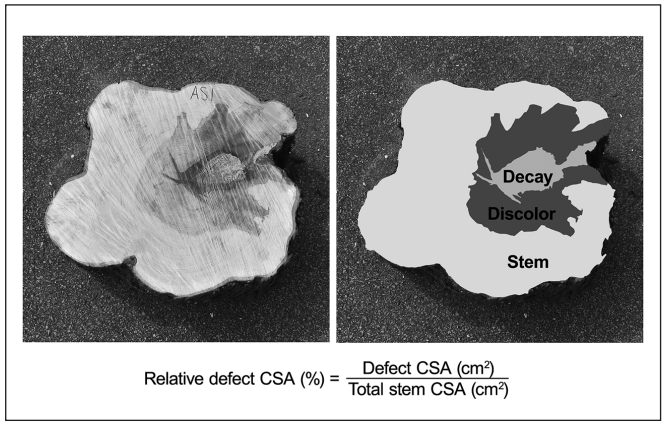

Figure 3. The relative amount of cross-sectional area occupied by a defect (relative defect CSA), represented as a percentage, was determined by dividing the surface area of the defect by that of the entire stem. In order to determine cross-sectional area, the perimeter of the stem and defect(s) were manually transferred onto a clear PVC transparency sheet, digitized, and analyzed using image processing software.

qualitative differences in trunk surface temperature distributions. The consistent temporal and spatial appearance of temperature anomalies was recorded, and these areas were compared with the observed external and measured internal stem characteristics.

Quantitative temperature readings were extracted from the images using two separate techniques. First, temperature data was extracted from the trunk surface within two rectangular transects positioned immediately above and below each other at the base

of the stem. The height of each transect was adjusted to equal twice the stem's diameter, measured 1 m above the ground (Figure 4). Statistical representation of transect surface temperature was derived using a measure of central tendency, the mean

[1] $$\bar{t} = \frac{\Sigma t_i}{n};$$

variability (viz. dispersion from the mean), the standard deviation

[2] $$s = \sqrt{\sum(t_i - \bar{t})^2 / n - 1};$$

and distribution symmetry, Pearson's skewness coefficient

[3] $$sk = \frac{\bar{t} - mode}{s},$$

within each transect. In these equations, t_i represents a temperature value at position i, $\bar{t}$ represents the mean temperature, and n represents the total number of temperature measurements within a transect.

Second, temperature data were extracted from the trunk along five parallel, vertical lines positioned equidistantly across the stem breadth (Figure 4). Surface temperature measurements extracted along each line were combined by averaging the measurements at each vertical position into a single column; this produced an approximation of the vertical temperature change along the 3 m trunk section. Temperatures extracted from individual stems were randomly checked for dissimilarities in trending imparted from emissivity measurement errors caused by the camera's viewing angle.

With these values, trunk surface temperature and relative defect CSA (%) were plotted together in a dual y-axis coordinate plane as a function of stem height for all trees in the experiment, allowing an evaluation of vertical changes in temperature alongside corresponding changes in internal condition (Figure 5). For each tree, a trend line was fitted to the trunk surface temperature using simple linear regression. At the trunk position nearest the maximum extent of internal defects, the difference between the surface temperature (point "A") and its trend line (point "B") was determined and recorded (Figure 5). This value ("deviation from linear trend") represented the magnitude of localized temperature anomalies near the position of internal defects relative to the general vertical temperature trend.

The linear relationship between relative defect CSA (%) and the statistical descriptions of surface temperature, including those extracted from rectangular transects (mean, standard deviation, skewness) and vertical linear plots (deviation from linear trend), were separately evaluated in scatterplots containing all trees and defect categories. Bivariate correlation analysis was subsequently used to assess the linear dependence of these variables using the Pearson correlation coefficient (r) and coefficient of determination (r^2). Multiple tests were conducted after separating the sampled stem sections into three representative groups according to their defect category, including 1) undamaged and discolored, 2) decayed and cavitated, and 3) decayed + discolored and cavitated + discolored. Finally, the suitability of simple, polynomial, or logarithmic linear regression models for this dataset was assessed based on the degree of dependence displayed in scatterplots and correlation statistics. All statistical tests were conducted in SPSS Statistics 19.0 for Windows (IBM Corp. 2010).

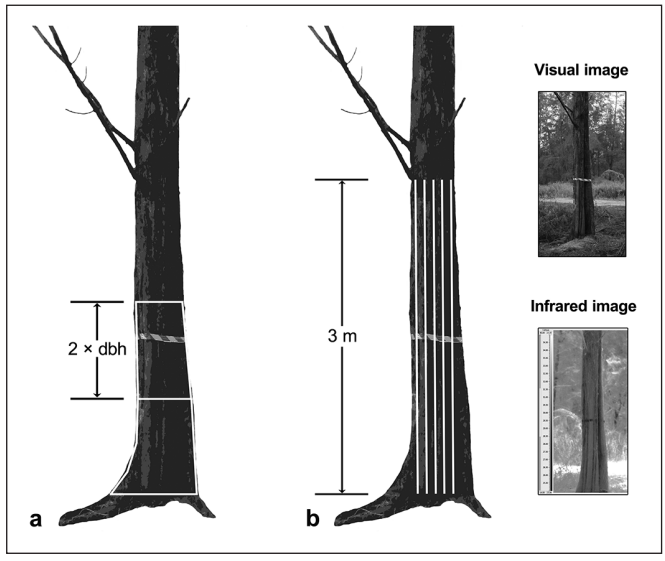

Figure 4. As shown in this diagram, temperature data was extracted from each tree using two separate methods. First, temperatures within vertically adjacent rectangular transects (a) were extracted for analysis. Second, temperature values were extracted along five lines equidistantly spaced across the stem breadth (b) and averaged into one linear trend line. Temperature values were then compared with the quality of internal stem tissue immediately beneath the area from which they were extracted.

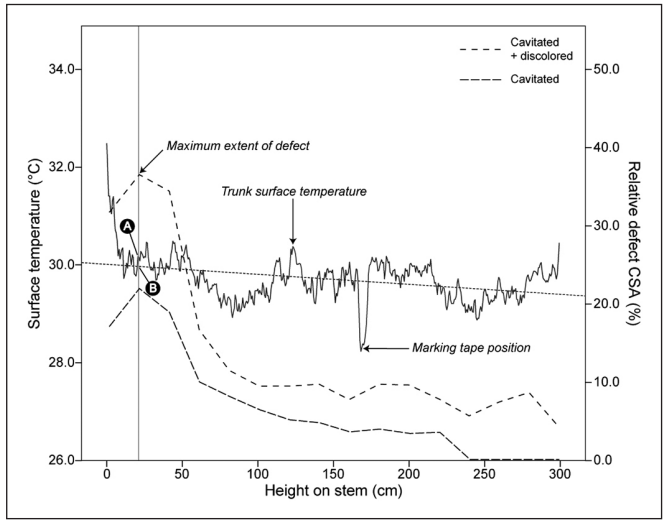

Figure 5. For each specimen, the relationship between vertical temperature changes and internal stem condition was summarized in a dual y-axis coordinate plane containing the trunk surface temperature (°C), extracted from five parallel vertical lines, and relative defect CSA (%) as a function of stem height (cm). As seen in the example from specimen J, the difference between the surface temperature (point "A") and its trend line (point "B") was assessed at the position containing the largest internal defect.

RESULTS

The physical dimensions of the 48 trees sampled for evaluation had an average diameter of 41.5 cm (SD 5.2) (measured at 1 m height) and average height of 35 m (SD 5.1) (Table 1). Climatic conditions during IR image collection were partly cloudy with temperatures ranging between 30°C and 32°C, 50%– 60% relative humidity, and winds out of the north northeast between 15 and 20 kph. There was no rainfall during IR image collection at the site.

After felling, visual assessment and physical measurement of destructively harvested stem cross sections revealed that three trees (6% of sample) contained internal termite-induced cavitations with associated fungal discoloration. These defects were characterized by irregularly shaped, smooth-walled voids surrounded by stiff discolored tissue and termites at all life stages (i.e., eggs, nymphs, adults) (Figure 2a). Among the affected sections, cavitated tissue occupied, on average, 5.1% of stem cross-sectional area (relative defect CSA). For these same sections, cavitated tissue with associated discoloration, in combination, averaged 16.6% relative defect CSA. The largest individual cross-sectional cavity occupied 21.8% relative defect CSA (Table 1).

Thirteen trees (27% of sample) contained fungal decay and discoloration. The decayed fungal lesions visibly modified the wood appearance with irregular color changes, darkened fungal interaction lines, and peripheral host reaction zones (Figure 2b). Penetrometer measurements confirmed the presence of decay with affected tissue permitting, on average, 9.2 mm (SD 21.0) greater axial penetration than proximal healthy tissue. Among the affected sections, decayed tissue occupied, on aver-

Table 1. Physical dimensions, including height and diameter (measured 1 m above ground) and cross-sectional area (CSA), of internal defects among 48 *Casuarina equisetifolia* sampled for this study.

				Maximum defect extent	
Tree ID	Diameter (cm)	Height (m)	Defect	Defect CSA (cm^2)	Relative defect CSA (%)
A	45.6	35.3	Decayed	39.7	3.5
B	46.4	30.8	Decayed	172.5	13.0
C	44.4	31.5	Decayed	86.7	7.0
D	51.7	42.4	Decayed	160.0	8.5
E	48.8	33.7	Discolored	240.5	18.0
F	42.1	34.3	Discolored	174.3	18.7
G	46.5	31.0	Discolored	215.3	18.0
H	43.8	34.5	Decayed	99.1	7.6
I	37.4	35.4	Cavitated	38.6	4.3
J	37.5	34.2	Cavitated	272.1	21.8
K	44.8	38.0	Discolored	328.1	22.4
L	44.6	49.2	Decayed	203.4	13.9
M	43.2	34.3	Discolored	477.8	54.9
N	46.3	23.7	Cavitated	86.9	3.6
O	53.2	37.6	Decayed	272.0	15.4
P	39.4	32.6	Discolored	149.2	17.2
Q	42.9	34.7	Discolored	331.0	34.5
R	37.1	37.2	Discolored	175.6	20.5
S	42.8	40.1	Decayed	44.8	3.7
T	38.7	26.1	Discolored	205.7	20.0
U	33.7	31.5	Discolored	112.8	17.3
V	41.2	39.1	Discolored	722.9	51.6
W	36.2	39.2	Decayed	13.7	1.8
X	33.3	36.1	Discolored	31.0	4.0
Y	33.6	35.8	Discolored	212.4	28.9
Z	31.3	29.1	Decayed	38.0	4.3
AA	38.2	36.0	Discolored	284.4	32.5
AB	43.8	30.5	Discolored	280.8	24.0
AC	45.2	34.5	Discolored	678.9	33.9
AD	43.3	43.7	Decayed	209.4	19.4
AE	35.9	32.9	Discolored	208.7	30.7
AF	36.3	36.1	Discolored	240.8	18.1
AG	34.3	36.7	Discolored	277.0	39.2
AH	42.7	32.5	Discolored	284.0	29.7
AJ	39.1	25.9	Discolored	652.6	37.6
AK	47.1	47.7	Discolored	314.3	30.4
AL	47.2	35.2	Discolored	489.2	21.9
AM	35.7	36.5	Discolored	329.4	25.3
AN	52.2	34.0	Discolored	642.8	39.4
AO	41.8	41.3	Discolored	314.7	16.2
AP	48.9	45.6	Discolored	754.3	32.2
AQ	34.8	31.5	Discolored	189.0	15.4
AR	40.1	31.8	Discolored	115.3	14.2
AS	43.4	34.0	Decayed	92.2	7.1
AU	41.3	29.5	Undamaged	-	-
AV	40.7	34.0	Discolored	159.8	8.9
AW	40.0	35.8	Discolored	219.7	13.6
AX	40.9	31.3	Decayed	82.6	5.6

age, 5.8% relative defect CSA. In combination, decayed tissue with associated discoloration averaged 25.8% relative defect CSA. The largest individual cross-sectional wood decay lesion occupied 19.4% relative defect CSA (Table 1). In 12 trees, the lesions were oriented axially and centered along the pith in a pattern typical of heart rot. In the one remaining tree, the lesions were locally positioned in the sapwood near external wounds, including those caused by brush fires and mechanical damage. All lesions expanded comparatively greater in the longitudinal direction compared to radial or circumferential directions. Among the wood decay lesions observed, longitudinal expansion was, on average, 15 times greater than radial expansion.

Thirty-one trees (62% of sample) exclusively contained fungal discoloration made apparent by irregular wood color changes and darkened fungal interaction lines (Figure 2c). In these sections, mechanical penetration resistance measurements did not yield impressions exceeding 1 mm outside the reference values. On average, discoloration accounted for 21.3% relative defect CSA among affected cross sections. The largest individual cross-sectional discolored area occupied 54.9% relative defect CSA (Table 1). One tree (2%) did not contain internal defects (Figure 2d; Table 1).

Qualitative evaluation of infrared images revealed regular associations between surface temperature anomalies and external stem features (Figure 6). Localized surface temperature reductions were spatially associated with mechanical damage, detached bark, cracks, termite nests, and shed branch wounds. Similar temperature reductions were frequently observed within concave surfaces lying between buttress roots, and the frequency of these anomalies was positively associated with buttress root formation and stem geometric irregularity. In addition, relatively low surface temperatures were consistently observed in a regular horizontal band across many tree stems (Figures 6a–d). Contrastingly, local and general surface temperature increases were observed on trees receiving direct, unfiltered solar radiation during infrared image collection. These trees were growing in relatively exposed or low-density forest areas, including the periphery of forest gaps and access roads. Similar temperature anomalies were absent on specimens growing in high-density forested areas (Figure 6e–f).

In visually comparing the surface temperature at locations determined to overlie concealed internal defects, consistent trends or anomalies in surface temperature were not observed. Sporadic temperature anomalies were visible on some trunk surfaces overlying defects, but the magnitude of temperature anomalies did not represent the size or position of internal decay or cavitation. Moreover, there was no obvious visual trend in surface temperature among trees with similar defects. Histo-

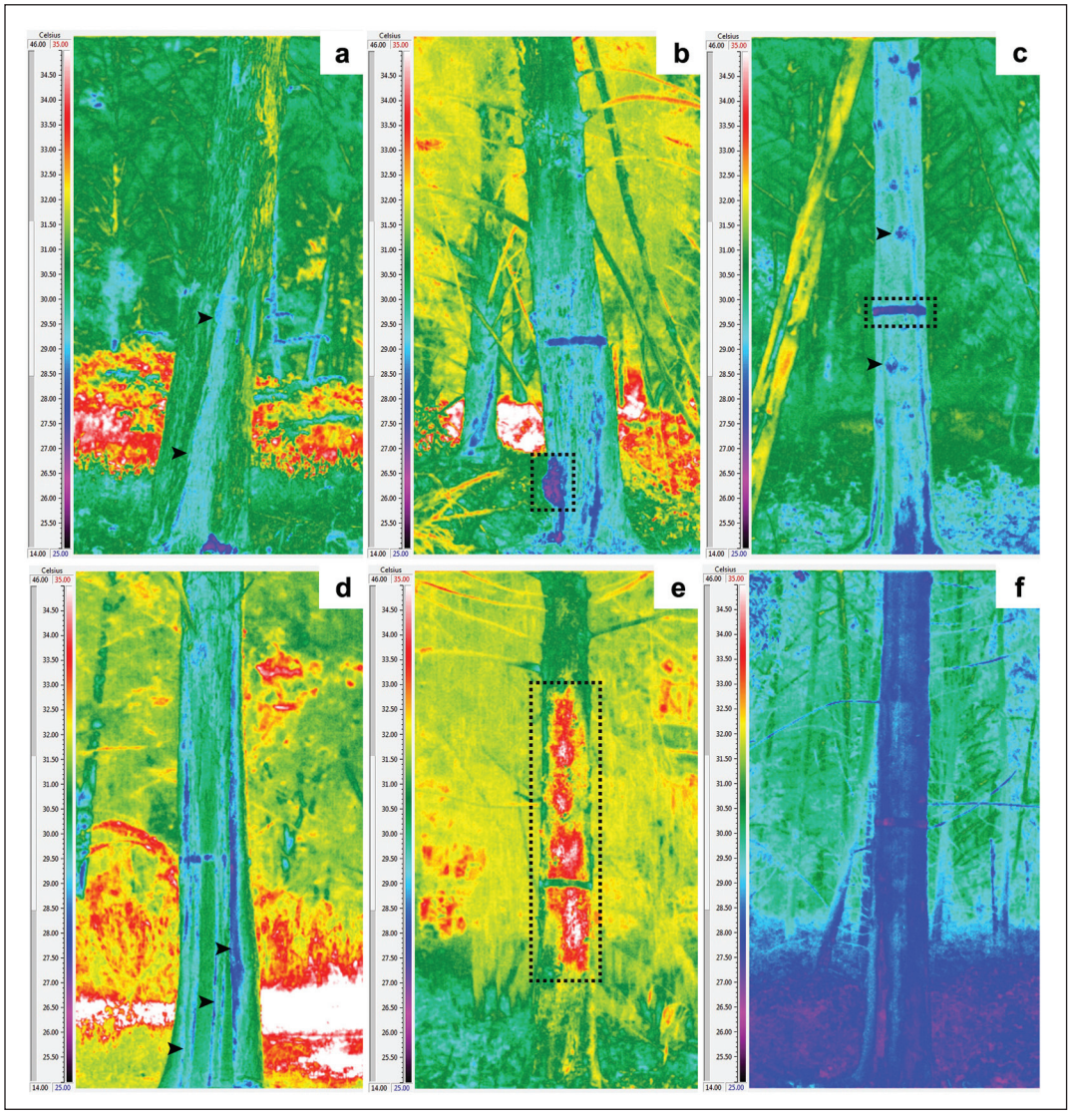

Figure 6. Qualitative IR image evaluation showed a consistent relationship between external stem features and temperature anomalies, particularly those caused by (a) detached bark, (b) termite nests, (c) branch wounds (arrows) and marking tape used to identify sampled specimens (black box), and (d) irregular stem geometry. Atmospheric conditions contributed to surface temperature anomalies, particularly for trees (e) growing in relatively exposed locations receiving direct, unfiltered solar radiation (black box). In contrast, specimens (f) growing in dense forested areas with low sunlight infiltration presented relatively homogenous surface temperature distributions.

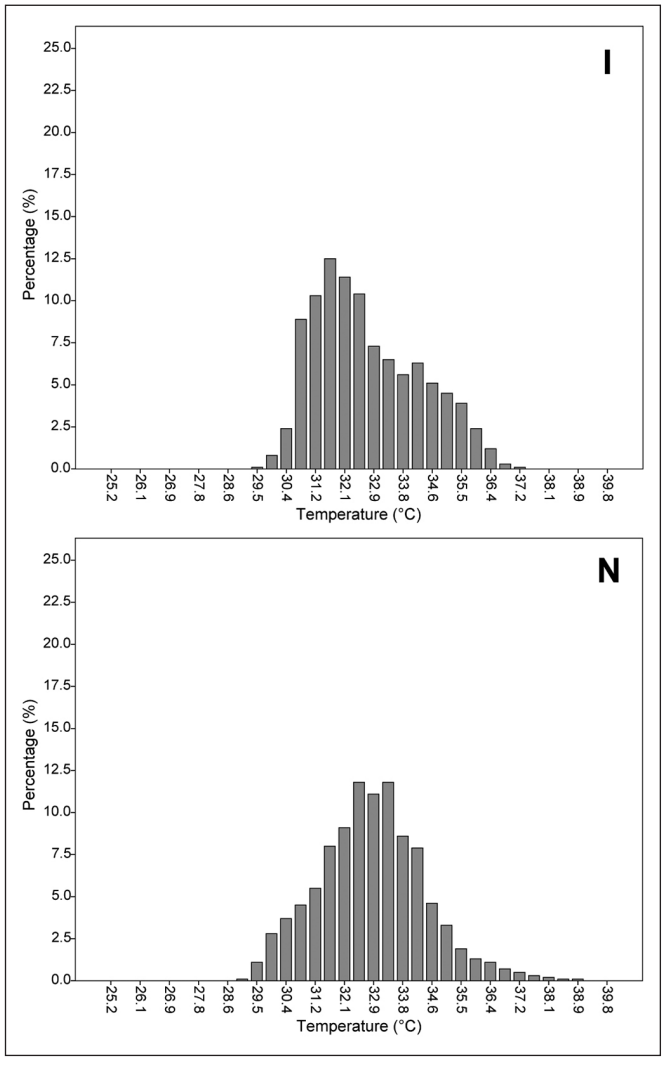

Figure 7. The two histograms, representing surface temperature distributions extracted from the trunk surface of trees "I" and "N," do not exhibit strong visual similarity, in spite of comparable internal cavity sizes.

grams displaying surface temperature distributions for trees with comparable defects were often visually dissimilar (Figure 7).

The size of the internal stem defects, represented by relative defect CSA (%), was weakly correlated (r^2 = 0.001- 0.022) with the three evaluated statistical representations of surface temperature extracted from rectangular transects. Scatterplots displaying the extent of internal defects and surface temperature mean, standard deviation, and skewness did not exhibit clear linear relationships or grouping among the plotted points (Figure 8a–d). After grouping the cases into three categories of similar defects, a significant but weak positive correlation (r^2 = 0.096, *P*-value = 0.011, d.f. = 66) was discovered between relative defect CSA and the standard deviation for the discolored and undamaged stem segments (Figure 8b). Among the remaining defect categories, linear correlation analyses of the relationship between internal defect CSA (%) and statistical representations of surface temperature (i.e., mean, standard deviation, skewness) did not yield significant results.

Vertical temperature plots for individual trees displayed sporadic localized temperature irregularities often disassociated with internal defects. The average deviation from the linear trend was relatively small (mean = 0.2°C) near internal defects for all trees in the experiment. In contrast, a large deviation (mean = 1.5°C) consistently occurred near the external marking tape used to mark forest specimens as experimental trees. Overall, the size of the internal defects, represented by relative defect CSA, was weakly correlated (r^2 = 0.018) with the localized deviation from the linear trend. The scatterplot displaying these two variables did not display clear linear relationships or grouping among the plotted points. The qualitatively categorized data similarly did not reveal significant relationships between the two variables (Figure 8d).

DISCUSSION

The frequency of discoloration, decay, and cavitation among the sampled *Casuarina equisetifolia* specimens is broadly congruent with similar reports of fungal infections and termite infestations in tree populations. Sudin et al. (1992) found 35.5% of six- to nine-year-old *Acacia mangium* (Leguminosae) specimens contained heart rot wood decay lesions and 4% contained termite infestations in commercial forestry plantations near Sabah, Malaysia. In this study, 27% of sampled trees were decayed and 6% contained termite infestations, and the existing reports, coupled with these findings, generally indicate that a considerable fraction of individuals among a species in natural and managed forests suffer wood decay infections and termite infestations.

The majority of trees sampled were exclusively discolored. Although a theory of succession has been postulated in which wood-inhabiting fungi and bacteria modify discolored wood to create an amenable substrate for wood decay fungi (Shigo 1972), the independent ability of wood decay fungi to degrade wood has since been illustrated (Rayner and Boddy 1988). As there is no evidence that discolored trees will inevitably become decayed, their identification during tree risk assessment is relatively unimportant.

Visual observation of IR images consistently showed the close association between temperature anomalies and external trunk features, suggesting that trunk surface temperature distributions are mostly products of external thermodynamic processes whose magnitude is affected, in turn, by such features as irregular stem geometry, cankers, bark damage, wounds, and surface cracks. Derby and Gates (1966), as well as Potter and Andresen (2002), attempted to model tree trunk temperature by characterizing the conditional input parameters affecting three external (convective heat exchange, solar radiative heating, infrared radiative exchange) and one internal (thermal conductivity) thermodynamic process. Their model simulations of trunk temperature distributions acknowledged the relative importance of the external environment over internal stem conditions in its theoretical design. Within this framework, changes in conductivity resulting from internal defects may affect surface temperatures, but they must compete with the rate and magnitude of temperature changes caused by the remaining thermodynamic processes at the surface. Presumably, the contributions of the external processes toward surface temperature distributions could be held constant or removed to selectively evaluate anomalies resulting from defect-related changes in thermal conductivity using these models, but they would require substantial computative improvement to accurately predict quantitative temperature changes across space and time (Potter and Andresen 2002). Without the ability to isolate the irrelevant contributions of these

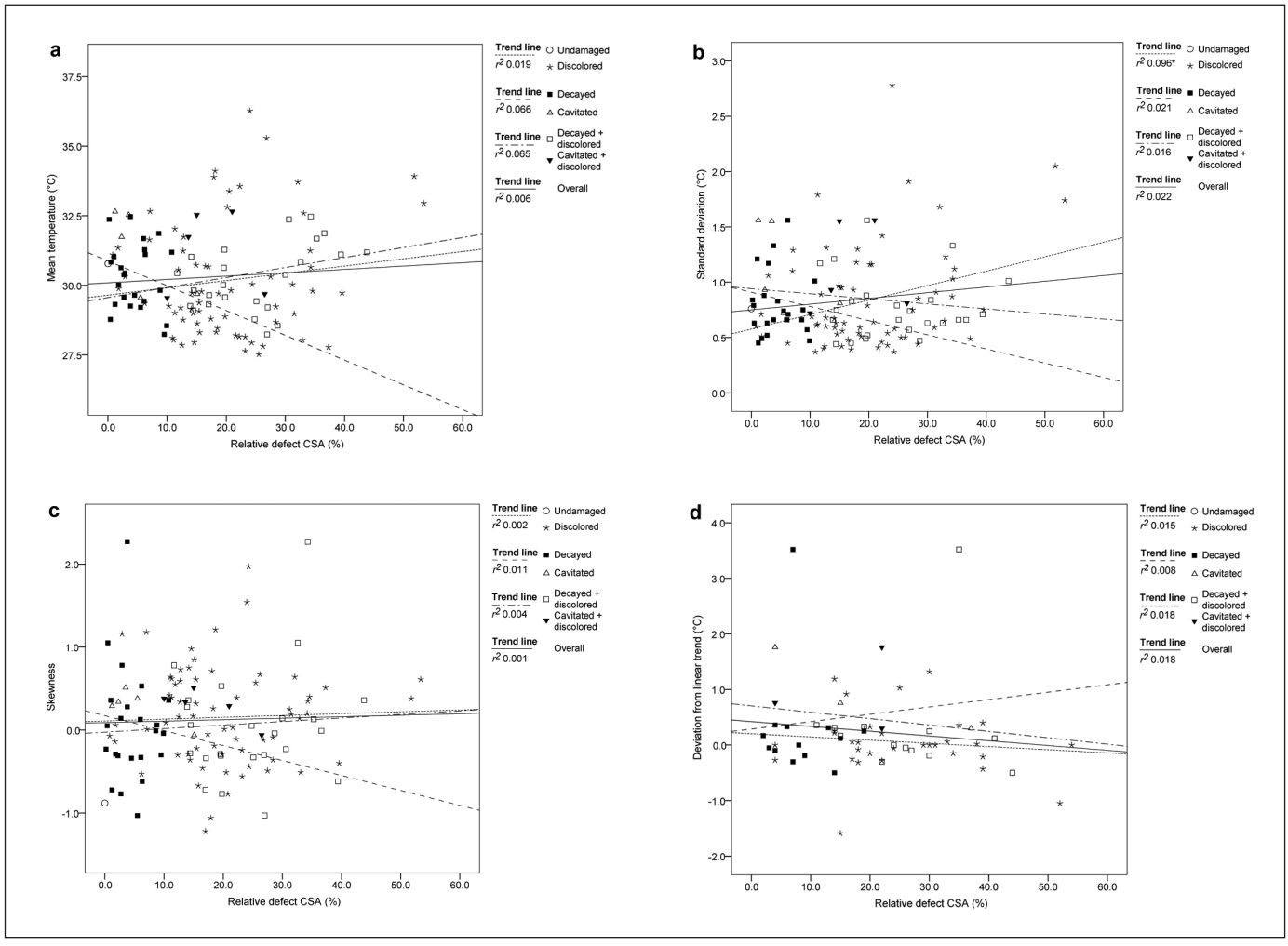

Figure 8. The internal condition of trees, represented by relative defect CSA, was compared with four different statistical representations of surface temperature, including the (a) mean, (b) standard deviation, (c) skewness, and (d) deviation from linear trend. The trees were categorized qualitatively based on their internal condition into one of six categories.

external processes towards surface temperature while attempting to assess internal condition, it may be increasingly difficult to establish a tree diagnostic technique with sufficient accuracy.

The differences in thermal emissivity among the diverse constituents of the trunk surface likely contributed additional surface temperature variability. The IR camera uses a preset emissivity value describing the target object's ability to emit infrared radiation within the 8–14 μm spectral range, coupled with infrared radiation received by the camera, to determine temperature values. Therefore, the technique is highly accurate when measuring surfaces with uniform thermal emissivity. The presence of moisture or epiphytic vegetation on the trunk surface will produce errors caused primarily by different emissivity of the materials. In this experiment, the phenomenon could be observed by the consistently lower temperatures associated with condensation accumulated underneath the marking tape, which was removed immediately before measurement (Figure 6c). Salisbury and D'Aria (1992) similarly reported variable spectral reflectance values, which can be used to predict thermal emissivity using Kirchhoff's Law, for interspecific tree bark, foliage, and epiphytic lichens. In the future, it would be important to characterize these values for common tree and epiphytic species.

Although external defects were not the focus of this study, it was apparent that the IR camera diagnostic technique consistently facilitated the identification of cracks, wounds, detached bark, and cankers. The consistency of these temperature anomalies around external defects allowed their reliable detection and identification in the IR images with minimal visual interpretation. The association of external defects and stem geometry with surface temperature anomalies, as well as the effect of sap flow on trunk surface temperature gradients, was reported in earlier studies (Burcham et al. 2011; Burcham et al. 2012). These findings suggest the camera may be especially useful for evaluating the vascular cambium and dermal tissues. Although the defects could be inspected with the IR camera, many qualified and experienced arborists could similarly assess them visually. The comparative accuracy, speed, and cost-effectiveness of an arborist's cognitive judgment would likely marginalize any utility gained by this particular application (Hickman et al. 1989; Hickman et al. 1995).

Qualitative observations and quantitative data analysis did not collectively reveal any meaningful relationship between a stem's internal condition and its surface temperature distribution. The infrared images did not portray consistent trends among trees containing similar defects, and the quantitative analysis tech-

niques failed to show any reliable connection between the statistical representations of surface temperature (mean, standard deviation, skewness, deviation from linear trend) and internal defects. Although one significant correlation was discovered between the amount of discoloration and surface temperature variability, similar results were not obtained for more severe defect categories.

For the range of internal defects encountered in this study, the IR camera diagnostic technique was unable to identify such cases distributed throughout the evaluated specimens. The largest defect encountered was a termite-induced cavity occupying, at one position, 21.8% stem cross-sectional area. The absence of defects measuring at least 76% stem cross-sectional area could be one explanation for the negative results obtained, as defects smaller than this have not been shown to produce a measureable temperature change (Burcham et al. 2012). Although the defects affecting these trees did not necessarily render individual specimens hazardous based on published criteria (Smiley and Fraedrich 1992; Kane and Ryan 2004), the defects were sufficiently large to serve as a calibration test for this diagnostic device. Based on existing literature, comparatively sized internal defects are detectable with a range of professional diagnostic tools, including resistance recording drills (Johnstone et al. 2007) and acoustic tomography devices (Gilbert and Smiley 2004).

CONCLUSION

This study demonstrated the difficulty encountered when interpreting and analyzing surface temperature measurements to assess internal stem condition. Surface temperature distributions displayed in the IR images of the 48 trees did not demonstrate a relationship with internal condition when analyzed using a mixed-methods approach. These results are practically important for the arboriculture professional community because they show the technique does not provide accurate results about the internal condition of trees containing decay and termite-induced cavitation up to and including the size of those encountered in this study (21.8% relative defect CSA). However, there was substantial evidence that surface temperature anomalies are regularly associated with damaged external stem tissue, and the camera may be useful in detecting cankers, detached bark, or mechanical damage.

LITERATURE CITED

Bellett-Travers, M., and S. Morris. 2010. The relationship between surface temperature and radial wood thickness of twelve trees harvested in Nottinghamshire. Arboricultural Journal 33:15–26.

Bo, M.W., J. Chu, and V. Choa. 2005. The Changi east reclamation project in Singapore. In: B. Indraratna, J. Chu, and J.A. Hudson (Eds.). Ground Improvement: Case Histories. Elsevier, Oxford, UK.

Burcham, D.C., E.C. Leong, and Y.K. Fong. 2012. Passive infrared camera measurements demonstrate modest effect of mechanically induced internal voids on *Dracaena fragrans* stem temperature. Urban Forestry & Urban Greening doi:10.1016/j.ufug.2012.01.001

Burcham, D.C., S. Ghosh, E.C. Leong, and Y.K. Fong. 2011. Evaluation of an infrared camera technique for detecting mechanically induced internal voids in *Syzygium grande*. Arboriculture & Urban Forestry 37(3):93–98.

Cartwright, K.S.G., and W.P.K. Findlay. 1958. Decay of timber and its prevention. HM Stationery Office, London. 332 pp.

Catena, A. 2003. Thermography reveals hidden tree decay. Arboricultural Journal 27:27–42.

Catena, A., and G. Catena. 2008. Overview of thermal imaging for tree assessment. Arboricultural Journal 30:259–270.

Catena, G., L. Palla, and M. Catalano. 1990. Thermal infrared detection of cavities in trees. European Journal of Forest Pathology 20:201–210.

Costello, L.R., and S.L. Quarles. 1999. Detection of wood decay in blue gum and elm: An evaluation of the Resistograph® and the portable drill. Journal of Arboriculture 25(6):311–318.

Dahle, G.A., and J.C. Grabosky. 2010. Variation in modulus of elasticity (E) along *Acer platanoides* L. (Aceraceae) branches. Urban Forestry & Urban Greening 9(3):227–233.

Derby, R.W., and D.M. Gates. 1966. The temperature of tree trunks – calculated and observed. American Journal of Botany 53(6):580–587.

Ellison, M.J. 2005. Quantified tree risk assessment used in the management of amenity trees. Journal of Arboriculture 31(2):57–65.

Fisher, J.B., and J.W. Stevenson. 1981. Occurrence of reaction wood in branches of dicotyledons and its role in tree architecture. Botanical Gazette 142(1):82–93.

Gilbert, E.A., and E.T. Smiley. 2004. Picus sonic tomography for the quantification of decay in white oak (*Quercus alba*) and hickory (*Carya* spp.). Journal of Arboriculture 30(5):277–281.

Harris, R.W., J.R. Clark, and N.P. Matheny. 2003. Arboriculture: Integrated management of landscape trees, shrubs, and vines (4th Edition). Prentice Hall, Englewood Cliffs, New Jersey, U.S. 592 pp.

Hickman, G., E. Perry, and R. Evans. 1995. Validation of a tree failure evaluation system. Journal of Arboriculture 21(5):23–34.

Hickman, G., J. Caprille, and E. Perry. 1989. Oak tree hazard evaluation. Journal of Arboriculture 15(8):177–184.

IBM, Corp., 2010. IBM® SPSS® Statistics Version 19.0. International Business Machines Corp., NewYork, New York, U.S.

James, K.R., N. Haritos, and P.K. Ades. 2006. Mechanical stability of trees under dynamic loads. American Journal of Botany 93(10):1522–1530.

Johnstone, D.M., G. Moore, M. Tausz, and M. Nicolas. 2010. The measurement of wood decay in landscape trees. Arboriculture & Urban Forestry 36(3):121–127.

Johnstone, D.M., P.K. Ades, G.M. Moore, and I.W. Smith. 2007. Predicting wood decay in eucalypts using an expert system and the IML-Resistograph drill. Arboriculture & Urban Forestry 33(2):76–82.

Kane, B.C.P., and H.D.P. Ryan III. 2004. The accuracy of formulas used to assess strength loss due to decay in trees. Journal of Arboriculture 30(6):347–356.

Kersten, W., and F.W.M.R. Schwarze. 2005. Development of decay in the sapwood of trees wounded by the use of decay detecting devices. Arboricultural Journal 28:165–181.

Larsson, B., B. Bengtsson, and M. Gustafsson. 2004. Nondestructive detection of decay in living trees. Tree Physiology 24:853–858.

Matheny, N.P., and J.R. Clark. 1994. A photographic guide to the evaluation of hazard trees in urban areas (2nd Edition). International Society of Arboriculture, Urbana. 85 pp.

Mattheck, C., and H. Breloer. 1994. The body language of trees: A handbook for failure analysis. The Stationery Office, London. 320 pp.

Nicolotti, G., P. Gonthier, F. Guglielmo, and M.M. Garbelotto. 2009. A biomolecular method for the detection of wood decay fungi: A focus on tree stability assessment. Arboriculture & Urban Forestry 35(1):14–19.

Ouis, D. 2003. Non-destructive techniques for detecting decay in standing trees. Arboricultural Journal 27:159–177.

Potter, B.E., and J.A. Andresen. 2002. A finite-difference model of temperatures and heat flow within a tree stem. Canadian Journal of Forest Research 32:548–555.

Rabe, C., D. Ferner, S. Fink, and F.W.M.R. Schwarze. 2004. Detection of decay in trees with stress waves and interpretation of acoustic tomograms. Arboricultural Journal 28:3–19.

Rayner, A.D.M., and L. Boddy. 1988. Fungal decomposition of wood: Its biology and ecology. John Wiley, Chichester, West Sussex, UK. 602 pp.

Salisbury, J.W., and D.M. D'Aria. 1992. Emissivity of terrestrial materials in the 8–14 μm atmospheric window. Remote Sensing of Environment 42:83–106.

Scheffer, T.C. 1936. Progressive effects of Polyporus versicolor on the physical and chemical properties of red gum sapwood. USDA Bulletin 527. Washington, D.C. 46 pp.

Schwarze, F.W.M.R. 2008. Diagnosis and prognosis of the development of wood decay in urban trees. ENSPEC, Rowville, Australia. 336 pp.

Schwarze, F.W.M.R., D. Lonsdale, and S. Fink. 1997. An overview of wood degradation patterns and their implications for tree hazard assessment. Arboricultural Journal 21:1–32.

Schwarze, F.W.M.R., J. Engels, and C. Mattheck. 2004. Fungal strategies of wood decay in trees. Springer-Verlag, Heidelberg, Germany. 185 pp.

Setten, G.G.K. 1953. The incidence of buttressing among Malayan tree species when of commercial size. Malayan Forester 16:219–221.

Shigo, A.L. 1972. Succession of microorganisms and patterns of discoloration and decay after wounding in red oak and white oak. Phytopathology 62:256–259.

Smiley, E.T., and B.R. Fraedrich. 1992. Determining strength loss from decay. Journal of Arboriculture 18(4):201–204.

Smiley, E.T., B.R. Fraedrich, and P.H. Fengler. 2000. Hazard tree inspection, evaluation, and management. pp. 243–260. In: J.E. Kuser (Ed.). Handbook of urban and community forestry in the Northeast. Kluwer Academic, New York, New York, U.S.

Sudin, M., S.S. Lee, and A.H. Harun. 1992. A survey of heart rot in some plantations of *Acacia mangium* in Sabah. Journal of Tropical Forest Science 6(1):37–47.

Thermoteknix. 2001. TherMonitor® Reporter System User Manual. Thermoteknix Systems Limited, Cambridge, England.

Watson, G. 2008. Discoloration and decay in severed tree roots. Arboriculture & Urban Forestry 34(4):260–264.

Wiemann, M.C., and G.B. Williamson. 1989. Radial gradients in the specific gravity of wood in some tropical and temperate trees. Forest Science 35:197–210.

Daniel C. Burcham (corresponding author)
Centre for Urban Greenery and Ecology
National Parks Board
Singapore 259569
daniel_burcham@nparks.gov.sg

Eng-Choon Leong
School of Civil and Environmental Engineering
Nanyang Technological University
Singapore 639798

Yok-King Fong
Centre for Urban Greenery and Ecology
National Parks Board
Singapore 259569

Puay-Yok Tan
School of Design and Environment
National University of Singapore
Singapore 117566

Résumé. L'évaluation des risques associés aux arbres est importante lorsque les communautés choisissent d'entretenir des arbres près des propriétés et des gens, et plusieurs outils peuvent être utilisés pour améliorer ces évaluations. L'efficacité dans la détermination de la condition interne de la tige d'un arbre en mesurant les températures à la surface du tronc au moyen de caméras infrarouges a été évaluée par cette étude. La température à la surface du tronc de 48 *Casuarina equisetifolia* a été évaluée; les arbres ont par la suite été abattus et débités afin de quantifier les défauts internes de la tige; une approche au moyen de méthodes mixes a enfin été employée pour déterminer la présence de défauts. Au total, 27% des arbres étaient cariés, 62% avaient du bois décoloré, 6% avaient des cavités infestées de termites et 2% n'avaient aucun défaut. L'évaluation qualitative visuelle des images infrarouges a permis de révéler une association intime entre les défauts externes de la tige avec les défauts internes au moyen de la distribution des températures à la surface. Des défauts externes, tels des chancres, des plaques d'écorce détachées et des dommages mécaniques ont été associés avec des anomalies de température. La condition interne de l'arbre avait un faible impact en terme de pourcentage sur la variabilité dans les mesures de température (r^2 = 0,0001 à 0,096). En conclusion, aucune relation évidente n'a été trouvée entre l'ampleur des défauts internes et la distribution des températures en surface. Ces résultats sont, de manière pratique, importants pour la communauté de l'arboriculture professionnelle parce qu'ils démontrent que cette technique ne permet pas de donner des résultats précis sur la condition interne des arbres.

Zusammenfassung. Die Untersuchung von Baumrisiken ist wichtig, wenn Kommunen Bäume auswählen, die in der Nähe von Ansiedlungen und Gebäuden gepflanzt werden. Viele Werkzeuge können genutzt werden, um die Untersuchungen zu unterstützen. In dieser Studie wird die Effektivität der Bestimmung von internen Stammverhältnissen durch Messung der Stammoberflächentemperatur mit Infrarotkameras untersucht. Die Oberflächentemperatur von 48 *Casuarina equisetifolia* –Stämmen wurde gemessen, die Bäume gefällt und zersägt, um die internen Stammdefekte zu quantifizieren. Zur Bestimmung der auftretenden Defekte wurden mehrere Ansätze kombiniert. Insgesamt waren 27 % der Bäume fäulebehaftet, 62 % waren verfärbt, 6 % waren durchlöchert von Termitenbefall und 2 % waren unversehrt. Qualitative visuelle Bewertungen der Infrarotaufnahmen enthüllten eine enge Relation externer Stammeigenschaften im Gegensatz zu internen Defekten, mit Schwankungen der Oberflächentemperatur. Externe Defekte wie Krebs, lose Rinde und mechanische Schäden wurden mit den Temperaturschwankungen assoziiert. Diese internen Baumbedingungen waren für einen kleinen Anteil an Variabilität der gemessenen Temperaturschwankungen (r^2 = 0,001-0,096) verantwortlich. Insgesamt wurden keine klaren Verhältnisse zwischen dem Ausmaß an internen Defekten und Oberflächentemperatur gefunden. Diese Ergebnisse sind praktisch wichtig für die Gemeinde der professionellen Arboristen, weil sie zeigen, dass die angewendete Technik keine akkuraten Ergebnisse über die interne Konditionen von Bäumen liefern kann.

Resumen. La evaluación del riesgo de los árboles es importante cuando las comunidades escogen cultivar los árboles cerca a la gente y las propiedades; muchas herramientas pueden ser usadas para mejorar estas evaluaciones. Fue probada en este estudio la efectividad de la determinación de la condición interna del tallo por la medición de las temperaturas superficiales del tronco con cámaras infrarrojas. Se evaluó la temperatura superficial del tronco de 48 *Casuarina equisetifolia*; los árboles fueron derribados y disectados para cuantificar los defectos internos del tronco; y una aproximación de varios métodos fue empleada para determinar la presencia de defectos. En total, 27% de los árboles estuvieron descompuestos, 62% decolarados, 6% con cavidad por infestación de termitas, y 2% sin daño. La evaluación cuantitativa visual de las imágenes infrarrojas reveló la asociación estrecha de características externas del tallo, en oposición a los defectos internos, con las distribuciones superficiales de la temperatura. Las características externas, tales como cancros, corteza abierta, y daño mecánico, estuvieron asociados con la temperatura. La condición interna de los árboles contabilizó para un pequeño porcentaje de la variabilidad en las mediciones de la temperatura (r2 = 0.001- 0.096). En total, no hay una relación clara entre la extensión de defectos internos y las distribuciones de la temperatura superficial. Estos resultados son importantes prácticamente para la comunidad profesional de la arboricultura debido a que muestran que la técnica no proporciona resultados precisos acerca de la condición interna de los árboles.